Arabian Journal of Chemistry (2013) 6, 211–223

King Saud University

Arabian Journal of Chemistry

www.ksu.edu.sa
www.sciencedirect.com

ORIGINAL ARTICLE

Xanthione: A new and effective corrosion inhibitor for mild steel in sulphuric acid solution

N.O. Obi-Egbedi [a], I.B. Obot [b,*]

[a] Department of Chemistry, University of Ibadan, Ibadan, Nigeria
[b] Department of Chemistry, Faculty of Science, University of Uyo, P.M.B. 1017, Uyo, Akwa Ibom State, Nigeria

Received 16 September 2010; accepted 2 October 2010
Available online 8 October 2010

KEYWORDS

Xanthione;
Mild steel corrosion inhibitors;
Density functional theory (DFT);
Sulphuric acid

Abstract The adsorption and inhibition effect of xanthione (XION) on mild steel in 0.5 M H_2SO_4 at 303–333 K were studied using gravimetric and UV–visible spectrophotometric methods. The results obtained show that XION acts as an effective corrosion inhibitor for mild steel in sulphuric acid and inhibition efficiency reaches 98.0% at a very low inhibitor concentration of 10 μM. Inhibition efficiency was found to increase with increase in XION concentration but decreased with temperature suggesting physical adsorption mechanism. Arrhenius law and its transition equation lead to estimate the activation parameters of the corrosion process. XION inhibits the corrosion of mild steel effectively at moderate temperature and adsorbs according to the Langmuir isotherm. Thermodynamic parameters governing the adsorption process have been calculated and discussed. The UV–visible absorption spectra of the solution containing the inhibitor after the immersion of mild steel specimen indicate the formation of a XEN–Fe complex. Attempt to correlate the molecular structure to quantum chemical indices was made using density functional theory (DFT).

1. Introduction

The study of organic compounds as acid corrosion inhibitors is a subject of immense interest due to their usefulness in several industrial applications such as pickling of metals, cleaning of boilers and acidification of oil wells (Abdallah and El-Naggar, 2001). An important method of protecting metallic materials against deterioration due to corrosion is by the use of inhibitors. The use of organic molecules as corrosion inhibitors is one of the most practical methods for protecting metals against corrosion and is becoming increasingly popular (Khaled et al., 2010; Obot et al., 2009; Obot and Obi-Egbedi, 2010a; Obot, 2009; Omar and Mokhtar, 2010; Fouda et al., 2010; Solmaz, 2010). Most of the well known acid inhibitors are aliphatic or aromatic compounds possessing nitrogen, sulphur and/oxygen atoms in their molecules. Furthermore, the presence of functional groups such as –N═N–, –CHO–, ═NH, R═R, and R–OH etc., aromaticity and electron density at donor atoms are found to influence the adsorption of inhibitor molecules on corroding metal surface (Pavithra et al., 2010; Obot and Obi-Egbedi, 2009).

* Corresponding author. Tel.: +234 8067476065.
E-mail address: proffoime@yahoo.com (I.B. Obot).

Peer review under responsibility of King Saud University.
doi:10.1016/j.arabjc.2010.10.004

Production and hosting by Elsevier

Xanthione and its derivatives are important class of compounds present in many chemical structures of great interest in a variety of biochemical and industrial field. They form structural elements of important classes of pharmaceutical drugs such as antimalarial, antifungal, antitumoral, antiallergic, anti-inflammatory and antiviral drugs (Ignatushchenko et al., 2000; Gopalakrishnan et al., 1997; Pedraza-Chaverri et al., 2008). Recently, we have reported on the effectiveness of xanthene and xanthone as inhibitors against the acid induced corrosion of mild steel in sulphuric acid (Obi-Egbedi and Obot, 2010; Obot and Obi-Egbedi, 2010b). The encouraging results obtained from these studies incited us to test more derivatives of this class of compounds. The choice of xanthione for the present investigation was based on the consideration that it contains several π-electrons including sulphur and oxygen heteroatoms, which can induce greater adsorption of the inhibitor molecule onto the surface of mild steel. Moreover, there is no report in the literature on the use of xanthione as corrosion inhibitor for mild steel in sulphuric acid.

In continuation of our quest for developing corrosion inhibitors with high effectiveness and efficiency, the present paper explore the use of xanthione as corrosion inhibitor for mild steel surface in sulphuric acid solution using gravimetric method. The effect of temperature on corrosion and inhibition processes are thoroughly assessed and discussed. Thermodynamic parameters governing the adsorption process were also calculated and discussed. UV–visible spectra were used to reveal the formation of inhibitor-Fe complex. Quantum chemical study using density functional theory (DFT) was further employed in an attempt to correlate the inhibitive effect with the molecular structure of xanthione.

2. Experimental method

2.1. Material

Tests were performed on a freshly prepared sheet of mild steel of the following composition (wt.%): 0.13% C, 0.18% Si, 0.39% Mn, 0.40% P, 0.04% S, 0.025% Cu, and bal Fe. Specimens used in the weight loss experiment were mechanically cut into 5.0 cm × 4.0 cm × 0.8 cm dimensions, then abraded with SiC abrasive papers 320, 400 and 600 grit, respectively, washed in absolute ethanol and acetone, dried in room temperature and stored in a moisture free dessicator before their use in corrosion studies (Obi-Egbedi and Obot, 2010).

2.2. Inhibitor

Xanthione (XION) was purchased from Sigma–Aldrich and used as inhibitor. Stock solution was made in 10:1 water:methanol mixture to ensure solubility (Ahamad and Quraishi, 2010). This stock solution was used for all experimental purposes. Fig. 1 shows the molecular structure of XION. It is evident that XION is a heterocyclic compound containing sulphur and oxygen atoms, which could easily be protonated in acidic solution, and several π-electrons exist in this molecule.

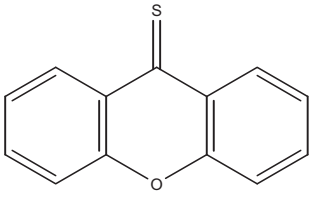

Figure 1 Molecular structure of xanthione (XION).

2.3. Solutions

The aggressive solutions, 0.5 M H_2SO_4 were prepared by dilution of analytical grade 98% H_2SO_4 with distilled water. The concentration range of XION prepared and used in this study was 2–10 μM.

2.4. Gravimetric measurements

The gravimetric method (weight loss) is probably the most widely used method of inhibition assessment (Musa et al., 2010; Khadom et al., 2010). The simplicity and reliability of the measurement offered by the weight loss method are such that the technique forms the baseline method of measurement in many corrosion monitoring programmes (Afidah and Kassim, 2008). Weight loss measurements were conducted under total immersion using 250 mL capacity beakers containing 200 mL test solution at 303–333 K maintained in a thermostated water bath. The mild steel coupons were weighed and suspended in the beaker with the help of rod and hook. The coupons were retrieved at 2 h interval progressively for 10 h, washed thoroughly in 20% NaOH solution containing 200 g/l of zinc dust (ASTM G1-72, 1990) with bristle brush, rinsed severally in deionized water, cleaned, dried in acetone, and re-weighed. The weight loss, in grammes, was taken as the difference in the weight of the mild steel coupons before and after immersion in different test solutions. Then the tests were repeated at different temperatures. In order to get good reproducibility, experiments were carried out in triplicate. In this present study, the standard deviation values among parallel triplicate experiments were found to be smaller than 5%, indicating good reproducibility.

The corrosion rate (ρ) in mg cm^{-2} h^{-1} was calculated from the following equation (Bentiss et al., 1999):

$$\rho = \frac{\Delta W}{At} \quad (1)$$

where W, is the average weight loss of three mild steel sheets; A, is the total area of one mild steel specimen, and t, is the

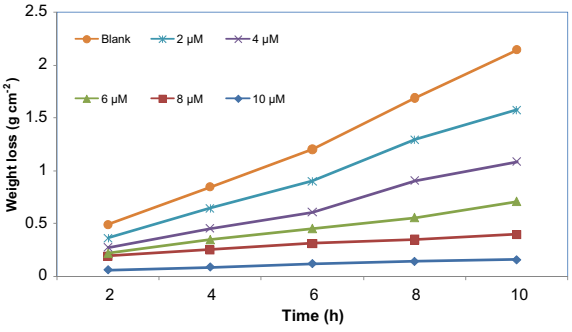

Figure 2 Variation of weight loss against time for mild steel corrosion in 0.5 M H_2SO_4 in the presence of different concentrations of XION at 303 K.

immersion time (10 h). With the calculated corrosion rate, the inhibition efficiency (%I) was calculated as reported previously (Umoren et al., 2009a,b):

$$\%I = \left(\frac{\rho_1 - \rho_2}{\rho_1}\right) \times 100 \quad (2)$$

where ρ_1 and ρ_2 are the corrosion rates of the mild steel coupons in the absence and presence of inhibitor, respectively.

2.5. Spectrophotometric measurements

UV–visible absorption spectrophotometric method was carried out on the prepared mild steel samples after immersion in 0.5 M H_2SO_4 with and without addition of 10 μM of xanthione at 303 K for three days. All the spectra measurements were carried out using a Perkin–Elmer UV–visible Lambda 2 spectrophotometer.

2.6. Computational details

B3LYP, a version of the DFT method that uses Becke's three parameter functional (B3) and includes a mixture of HF with DFT exchange terms associated with the gradient corrected correlation functional of Lee, Yang and Parr (LYP) (Lee et al., 1988), was used in this paper to carry out quantum calculations. Then, full geometry optimization together with the vibrational analysis of the optimized structures of the inhibitor was carried out at the (B3LYP/6-31G (d) level of theory using Spartan'06 V112 program package (Spartan and Wavefunction, 2006) in order to determine whether they correspond to a maximum or a minimum in the potential energy curve. The theoretical parameters were calculated for molecules in neutral as well as in the protonated form for comparison. It is well known that the phenomenon of electrochemical corrosion occurs in liquid phase. As a result, it was necessary to include the effect of a solvent in the computational calculations. In the Spartan'06 V112 program, SCRF methods (Self-consistent reaction field) were used to perform calculations in solution. These methods model the solvent as a continuum of uniform dielectric constant and the solute is placed in the cavity within it.

3. Results and discussion

3.1. Weight loss measurements

Weight loss of mild steel, in g cm^{-2} h^{-1}, was determined at various time intervals in the absence and presence of different concentrations of xanthione. Fig. 2 shows the weight loss-time curves obtained for mild steel in 0.5 M H_2SO_4 in the absence and presence of different concentrations of XION at 303 K. The figure shows that the presence of inhibitor falls significantly below that of free acid. Similar curves were obtained for 313–333K (not shown). The calculated values of corrosion rates (ρ) and inhibition efficiency (%I) obtained from weight loss measurements for different concentrations of xanthione in 0.5 M H_2SO_4 after 10 h immersion at 303–333 K are listed in Table 1. It is evident from this table and Fig. 3 that the corrosion rate decreased with increasing inhibitor concentration but increased with rise in temperature. Table 1 also shows that inhibition efficiency (%I) increased with increasing inhibitor concentration, reaching a maximum of 98.0%. This may be due to the adsorption of xanthione onto the mild steel surface through non-bonding electron pairs of sulphur and oxygen atoms as well as the π-electrons of the aromatic rings. The high inhibitive performance of xanthione suggests a higher bonding ability of the inhibitor to the mild steel surface. Similar observation has been reported (Ahamad and Quraishi, 2010). Furthermore, the inhibition efficiency values obtained for xanthione were higher when compared to that of xanthene and xanthone already reported in literature (Obi-Egbedi and Obot, 2010; Obot and Obi-Egbedi, 2010b).

3.2. Effect of temperature

The effect of temperature on the inhibited acid-metal reaction is very complex according to Bentiss et al. (2005), because many changes occur on the metal surface such as rapid etching, desorption of inhibitor and the inhibitor itself may undergo decomposition. The influence of temperature on percentage inhibition efficiency was studied by conducting weight loss

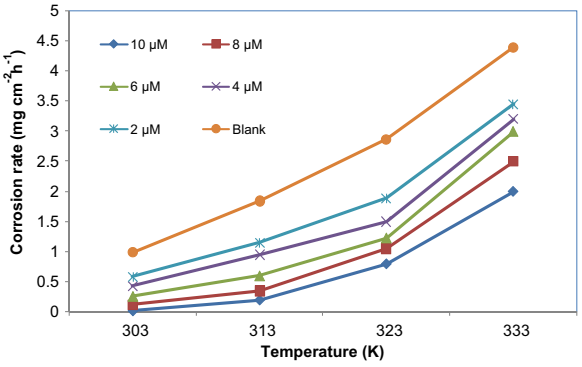

Figure 3 The relationship between corrosion rate and temperature for different concentrations of XION.

Table 1 Calculated values of corrosion rate and inhibition efficiency for mild steel corrosion for mild steel in 0.5 M H_2SO_4 in the absence and presence of XION at 303–333 K.

System/concentration (μM)	Corrosion rate (mg cm^{-2} h^{-1})				Inhibition efficiency (%I)			
	303 K	313 K	323 K	333 K	303 K	313 K	323 K	333 K
Blank	0.99	1.84	2.87	4.40	–	–	–	–
2	0.59	1.15	1.89	3.45	40.2	37.4	34.1	21.6
4	0.43	0.95	1.50	3.20	56.5	48.0	45.4	27.3
6	0.26	0.60	1.23	3.00	73.7	67.4	57.1	31.8
8	0.12	0.35	1.05	2.50	87.8	80.9	63.4	43.2
10	0.02	0.20	0.80	2.00	98.0	89.1	72.1	54.5

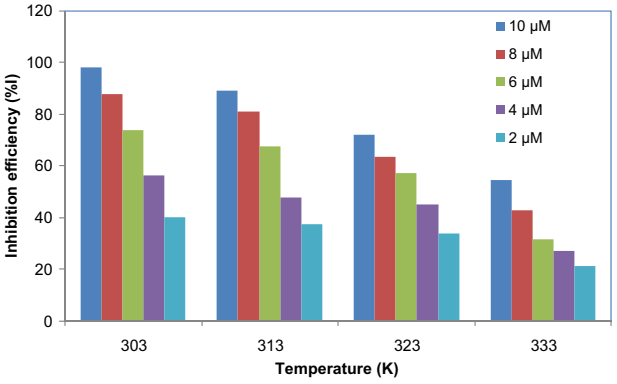

Figure 4 Variation of inhibition efficiency of XION with temperature.

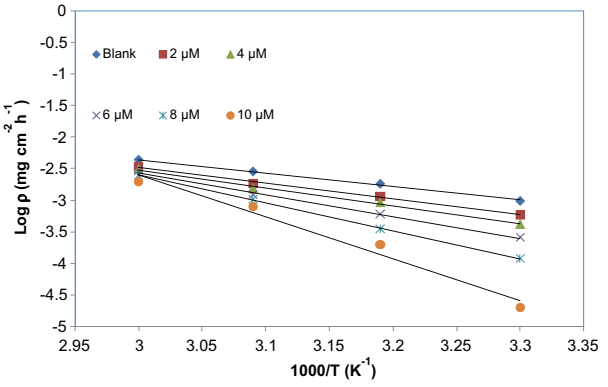

Figure 5 Arrhenius plot for mild steel corrosion in 0.5 M H_2SO_4 in the absence and presence of different concentrations of xanthione (XION).

measurements at 303–333 K containing different concentrations of XION (Table 1). Fig. 4 shows the variation of percentage inhibition efficiency with temperature. It is clear from the figure that percentage inhibition efficiency increases with XION concentration but decreases with temperature. The decrease in inhibition efficiency with increase in temperature may be probably due to increased rate of desorption of XION from the mild steel surface at higher temperature (Li et al., 2010; Obot and Obi-Egbedi, 2010b).The relationship between the corrosion rate (ρ) of mild steel in acidic media and temperature (T) is often expressed by the Arrhenius equation (Behpour et al., 2009):

Table 2 Activation parameters of the dissolution of mild steel in 0.5 M H_2SO_4 in the absence and presence of different concentrations of XION.

C (M) (μM)	E_a (kJ mol^{-1})	ΔH^* (kJ mol^{-1})	ΔS^* (J mol^{-1} K^{-1})
Blank	4.07	17.92	−313.39
2	4.81	20.25	−318.28
4	5.42	22.57	−317.89
6	6.68	26.74	−315.79
8	8.48	32.72	−311.86
10	12.64	46.75	−296.07

$$\log \rho = \log A - \frac{E_a}{2.303RT} \quad (3)$$

where ρ, is the corrosion rate E_a, is the apparent activation energy, R, is the molar gas constant (8.314 J K^{-1} mol^{-1}), T, is the absolute temperature, and A, is the frequency factor. The plot of $log\ \rho$ against $1/T$ for mild steel corrosion in 0.5 M H_2SO_4 in the absence and presence of different concentrations of XION is presented in Fig. 5. All parameters are given in Table 2. It is clear that the addition of XION to the acid solution increases the value of E_a. The increase in E_a is proportional to the inhibitors concentration. Such a trend suggests that the corrosion reaction will be further pushed to the surface sites that are characterized by progressively higher values of E_a as the concentration of the inhibitor becomes larger (Mansfeld, 1987). This means that the adsorption of XION on mild steel surface leads to the formation of barrier layer that retards the metal activity in the electrochemical reactions of corrosion. Szauer and Brand (1981) explained that the increase in activation energy can be attributed to an appreciable decrease in the adsorption of the inhibitor on the mild steel surface with increase in temperature and a corresponding increase in corrosion rates due to the fact that greater area of metal is exposed to the acid environment. As adsorption decreases, more desorption of inhibitor molecules occurs because these two opposite processes are in equilibrium. Due to more desorption of inhibitor molecules at higher temperatures, the greater surface area of mild steel comes in contact with aggressive environment, resulting in an increase of corrosion rates with temperature. With high inhibitor concentrations, this problem is avoided because the degrees of surface coverage are close to saturation (Herrag et al., 2010). The increase in activation energy after the addition of XION to 0.5 M H_2SO_4 solution can indicate that physical adsorption (electrostatic interaction) occurs in the first stage (Solmaz et al., 2008a). Indeed XION molecule which contains O and S atoms in its structure can be protonated to form cation forms in acid medium. It is logical to assume that in this case the electrostatic cation adsorption is responsible for the good protective properties of this compound. However, the adsorption phenomenon of an organic molecule is not considered only as a physical or as chemical adsorption phenomenon. A wide spectrum of conditions, ranging from the dominance of chemisorption or electrostatic effects arises from other adsorption experimental data (Solmaz et al., 2008b).

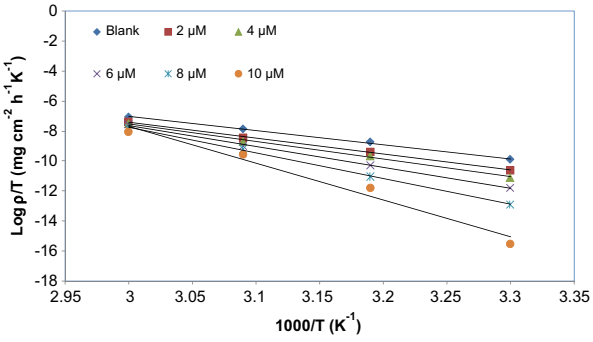

Figure 6 Transition state plot for mild steel corrosion in 0.5 M H_2SO_4 in the absence and presence of different concentrations of xanthione (XION).

Experimental corrosion rate values obtained from weight loss measurements for mild in 0.5 M H_2SO_4 in the absence and presence of XION was used to further gain insight on the change of enthalpy (ΔH^*) and entropy (ΔS^*) of activation for the formation of the activation complex in the transition state using transition equation (Bockris and Reddy, 1977):

$$\rho = \left(\frac{RT}{Nh}\right)\exp\left(\frac{\Delta S^*}{R}\right)\exp\left(\frac{-\Delta H^*}{RT}\right) \quad (4)$$

where ρ, is the corrosion rate; h, is the Plank's constant (6.626176×10^{-34} Js); N, is the Avogadro's number (6.02252×10^{23} mol^{-1}); R is the universal gas constant and T, is the absolute temperature. Fig. 6 shows the plot of log ρ/T versus $1/T$ for mild steel corrosion in 0.5 M H_2SO_4 in the absence and presence of different concentrations of XION. Straight lines were obtained with slope of ($\Delta H^*/2.303R$) and an intercept of [log (R/Nh) + ($\Delta S^*/2.303R$)] from which the values of ΔH^* and ΔS^*, respectively, were computed and listed also in Table 2. Inspection of these data reveals that the ΔH^* values for dissolution reaction of mild steel in 0.5 M H_2SO_4 in the presence of XION are higher (20.25–46.75 kJ mol^{-1}) than that in the absence of XION (17.92 kJ mol^{-1}). The positive sign of ΔH^* reflects the endothermic nature of the mild steel dissolution process suggesting that the dissolution of mild steel is slow (Guan et al., 2004). It is also clear from Table 2 that E_a and ΔH^* increase with increase in XION concentration.

Entropy of activation, ΔS^* remains almost constant with increasing XION concentration (Table 2) and their values were negative both in the uninhibited and inhibited systems. The negative values of entropies of activation imply that the activated complex in the rate determining step represents an association rather than a dissociation step, meaning that a decrease in disordering takes place on going from reactants to the activated (Herrag et al., 2010).

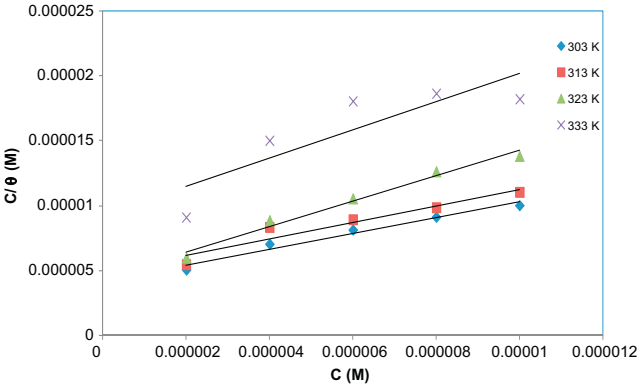

Figure 7 Langmuir adsorption plot for mild steel in the presence of XION.

Table 3 Some parameters from Langmuir adsorption isotherm for mild steel in 0.5 M H_2SO_4 in the presence of XION.

Temperature (K)	R^2	K_{ads} (M^{-1})	ΔG^o_{ads} (kJ mol^{-1})	Slope
303	0.970	2.5×10^4	−41.4	0.605
313	0.917	2.0×10^5	−42.2	0.635
323	0.980	2.2×10^5	−44.1	0.980
333	0.742	1.1×10^5	−43.2	1.090

3.3. Adsorption isotherm

It is well recognized that the first step in inhibition of metallic corrosion is the adsorption of organic inhibitor molecules at the metal/solution interface. Furthermore, the adsorption depends on the molecule's chemical composition, the temperature and the electrochemical potential at the metal/solution interface. So the adsorption of organic inhibitor molecules from the aqueous solution can be regarded as a quasi-substitution process between the organic compounds in the aqueous phase [$Org_{(sol)}$] and water molecules at the electrode surface [$H_2O_{(ads)}$] (Sahin et al., 2002):

$$Org_{(sol)} + xH_2O_{(ads)} \leftrightarrow Org_{(ads)} + xH_2O_{(sol)} \quad (5)$$

where x is the size ratio, that is, the number of water molecules replaced by one organic inhibitor. Basic information on the interaction between the inhibitor of the mild steel surface can be provided by the adsorption isotherm. In order to obtain the isotherm, the linear relation between degree of surface coverage (θ) values (θ = %I/100) and inhibitor concentration (C) must be found. Attempts were made to fit the θ values to various isotherms including Langmuir, Temkin, Frumkin and Flory–Huggins. By far the best fit was obtained with the Langmuir isotherm. This model has also been used for other inhibitor systems (Kissi et al., 2006; Machnikova et al., 2008). According to this isotherm, θ is related to C by:

$$\frac{C}{\theta} = \frac{1}{K_{ads}} + C \quad (6)$$

where K_{ads} denotes the equilibrium *constant* for the adsorption process.

Fig. 7 shows the plots of C/θ versus C and the expected linear relationship is obtained with good correlation coefficients confirming the validity of the equation. The slopes were less than unity at 303 and 313 K except in the case of 323 and 333 K where the value of the slope was 0.98 and 1.09, respectively, which is an indication that the Langmuir isotherm is obeyed at these temperatures (Table 3). The considerable deviation of the slope from unity observed at 303 and 313 K may be explained on the basis of the interaction among the adsorbed species on the surface of the metal (Obot et al., 2009). It is therefore pertinent to say that the adsorption of XION on the mild steel surface at 303 and 313 K can be more appropriately represented by a modified Langmuir equation suggested by Villamil et al. (1999) taking into consideration the interactions between adsorbate species as well as changes in heat of adsorption with changing surface coverage as follows:

$$\frac{C}{\theta} = \frac{n}{K_{ads}} + nC \quad (7)$$

The values of equilibrium constant of adsorption K_{ads} obtained from the Langmuir adsorption isotherm are listed in Table 3, together with the values of the Gibbs free energy of adsorption (ΔG^o_{ads}) calculated from the equation:

$$\Delta G^o_{ads} = -RT\ln(55.5K_{ads}) \quad (8)$$

where R is the universal gas constant; T, *is* the thermodynamic temperature and the value of 55.5 is the concentration of water in the solution expressed in molar.

The high values of K_{ads} for studied XION indicate stronger adsorption on the mild steel surface in 0.5 M H_2SO_4 solution. This can be explained by the presence of sulphur, oxygen heteroatoms and π-electrons in the inhibitor molecule. It has been reported that the higher the K_{ads} value (>100 M^{-1}), the stronger and more stable the adsorbed layer of the inhibitor on metal surface and consequently, the higher the inhibition efficiency (Lagrenee et al., 2002). These data support the good performance of XION as corrosion inhibitor for mild steel in 0.5 M H_2SO_4 solution.The negative values of ΔG^o_{ads}, calculated from Eq. (8), are consistent with the spontaneity of the adsorption process and the stability of the adsorbed layer on the steel surface. Generally, values of ΔG^o_{ads} up to -20 kJ mol^{-1} are consistent with physisorption, while those around -40 kJ mol^{-1} or higher are associated with chemisorption as a result of the sharing or transfer of electrons from organic molecules to the metal surface to form a coordinate bond (Donahue and Nobe, 1965). In the present study, the calculated values of ΔG^o_{ads} obtained for XION ranges between -32.1 and -42.1 kJ mol^{-1} (Tables 3 and 4), indicating that the adsorption of mechanism of XION on mild steel in 0.5 M H_2SO_4 solution at the studied temperatures may be a combination of both physisorption and chemisorption (comprehensive adsorption) (Ahamad et al., 2010). However, physisorption was the major contributor while chemisorption only slightly contributed to the adsorption mechanism judging from the decrease of $\%I$ with increase in temperature and the higher values of E_a obtained in the presence of inhibitor when compared to its absence.

Table 4 Some parameters from statistical model for mild steel in 0.5 M H_2SO_4 in the presence of XION.

Temperature (K)	R^2	θ	ΔG^o_{ads} (kJ mol^{-1})
303	0.949	1.04×10^3	−32.1
313	0.993	1.58×10^3	−32.8
323	0.989	2.73×10^3	−33.1
333	0.975	3.21×10^3	−33.7

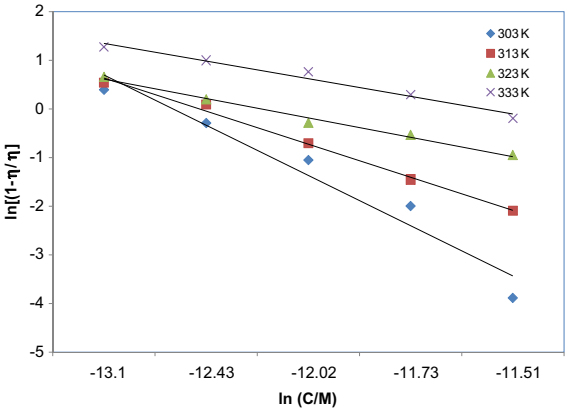

Figure 8 Application of the statistical model to the corrosion protection behavior of xanthione.

3.4. Thermodynamic consideration using the statistical model

The adsorption of an inhibitor species, I, on a metal surface, M, can be represented by a simplified equation:

$$M + I \leftrightarrow M(I)_{\text{ads}} \tag{9}$$

Let M of the above reaction be the system in the ensemble and the solvent containing inhibitor molecules as donor particles be the medium. The complex-forming process can be regarded as the course of distribution of donor particles to the system. So it is justifiable to extend the model of variable number of particles in statistical physics for the inhibiting process.

According to statistical physics (Landau and Lifshitz, 1980), the change of free energy of adsorption ΔG^o_{ads} can be calculated from Eq. (10) as follows (Wang et al., 2002; Obi-Egbedi and Obot, 2010; Obot and Obi-Egbedi, 2010b):

$$\ln\left(\frac{1-\eta}{\eta}\right) = \frac{\Delta G^o_{ads}}{\theta} - \frac{RT\ln C}{\theta} \tag{10}$$

where C is the concentration of inhibitor particles.

The curve fitting of data in Table 1 to the statistical model at 303–333 K is presented in Fig. 8. Good correlation coefficient ($R^2 > 0.94$) was obtained. θ and ΔG^o_{ads} can be calculated from the slope and intercept of Eq. (10). All the calculated parameters are given in Table 4. The values of ΔG^o_{ads} obtained from Statistical Physics and that obtained from the last approach (Eq. (8)) show close correlation.

The enthalpy of adsorption can also be calculated from the Gibbs–Helmholtz equation (Singh and Quraishi, 2010):

$$\left[\frac{\partial(\Delta G^o_{ads}/T)}{\partial T}\right]_p = -\frac{\Delta H^o_{ads}}{T^2} \tag{11}$$

Eq. (11) can be arranged to give the following equation:

$$\frac{\Delta G^o_{ads}}{T} = \frac{\Delta H^o_{ads}}{T} + k \tag{12}$$

The variation of $\Delta G^o_{ads}/T$ with $1/T$ gives a straight line with a slope which is equal to ΔH^o_{ads} (Fig. 9). It can be seen from the figure that $\Delta G^o_{ads}/T$ decreases with $1/T$ in a linear fashion. The obtained value of ΔH^o_{ads} was -16.18 kJ mol^{-1}.

The enthalpy and entropy for the adsorption of XION on mild steel were also deduced from the thermodynamic basic equation (Bouklah et al., 2006):

$$\Delta G^o_{ads} = \Delta H^o_{ads} - T\Delta S^o_{ads} \tag{13}$$

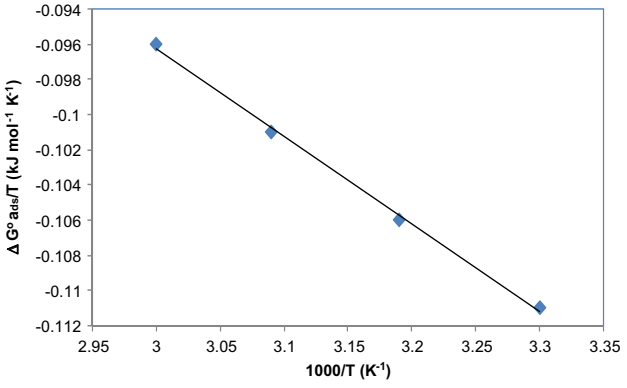

Figure 9 The variation of $\Delta G^o_{ads}/T$ with $1/T$.

where ΔH^{o}_{ads} and ΔS^{o}_{ads} are the enthalpy and entropy changes of adsorption process, respectively. A plot of ΔG^{o}_{ads} versus T was linear (Fig. 10) with the slope equal to $-\Delta S^{o}_{ads}$ and intercept of ΔH^{o}_{ads}. The enthalpy of adsorption ΔH^{o}_{ads}, and the entropy of adsorption ΔS^{o}_{ads}, obtained are $-16.00\ \mathrm{kJ\ mol^{-1}}$ and $-52.00\ \mathrm{J\ mol^{-1}\ K^{-1}}$, respectively. The negative sign of ΔH^{o}_{ads} indicates that the adsorption of XION molecules is an exothermic process. In an exothermic process, physisorption is distinguished from chemisorption by considering the absolute value of ΔH^{o}_{ads}. For physisorption process, the enthalpy of adsorption is lower than 40 kJ $\mathrm{mol^{-1}}$ while that for chemisorption approaches 100 kJ $\mathrm{mol^{-1}}$ (Singh and Quraishi, 2010). In the present study, the absolute value of enthalpy of adsorption obtained is typical of physisorption. Values of ΔH^{o}_{ads} obtained by the two methods are in good agreement.

The entropy of adsorption obtained from Eq. (13) was negative because inhibitor molecule freely moving in the bulk solution (inhibitor molecule were chaotic), were adsorbed in an orderly fashion onto the mild steel, resulting in a decrease in entropy (Li et al., 2010). Moreover, from thermodynamic principles, since the adsorption was an exothermic process, it must be accompanied by a decrease in entropy (Noor and Al-Moubaraki, 2008).

3.5. UV–visible spectroscopy

A substantial support for the formation of metal complex is often obtained by UV–visible spectroscopic investigation. Since there is often a certain quantity of metal cation in the solution that is first dissolved from the metal surface, such procedures were conducted in the present work to confirm the possibility of the formation of [XION–Fe^{2+}] complexes as described in several publications (Sherif and Park, 2005; Rangelov and Mircheva, 1996; Elmorsi and Hassanein, 1999; Abdel-Gaber et al., 2009). Futhermore, Abboud et al. (2007) have reported that change in position of the absorbance maximum and change in the value of absorbance indicate the formation of a complex between two species in solution.

In order to confirm the possibility of the formation of XION–Fe complex, UV–visible absorption spectra obtained from 0.5 M H_2SO_4 solution containing 10×10^{-6} M XION before and after three days of mild steel immersion are shown in Fig. 11. The electronic absorption spectra of XION before the steel immersion display a main visible band at 380 nm. This band may be assigned to π–π* transition involving the whole electronic structure system of the compound with a considerable charge transfer character (Abboud et al., 2009). After three days of steel immersion (Fig. 11), it is clearly seen that the band maximum underwent a blue shift, suggesting the interaction between XION and Fe^{2+} ions in the solution (Abboud et al., 2007). Futhermore, there is an increase in the absorbance of this band. It is clear that there was no significant difference in the shape of the spectra before and after the immersion of XION showing a possibility of weak interaction between XION and mild steel (physisorption). These experimental findings give a strong evidence for the posibility of the formation of a complex between Fe^{2+} cation and XION in 0.5 M H_2SO_4.

3.6. Quantum chemical studies

Recently, the density functional theory (DFT) has been used to analyze the characteristics of the inhibitor/surface mechanism and to describe the structural nature of the inhibitor on the corrosion process (Lashkari and Arshadi, 2004; Sein et al., 2001; Ebenso et al., 2010). Furthermore, DFT is considered as a very useful technique to probe the inhibitor/surface interaction as well as to analyze the experimental data. Thus in the present investigation, quantum chemical calculation using DFT was employed to explain the experimental results obtained in this study and to further give insight into the inhibition action of XION on the mild steel surface.

Figs. 12–15 show the optimized geometry, the HOMO density distribution, the LUMO density distribution and the Mulliken charge population analysis plots for XION molecule obtained with DFT at B3LYP/6-31G (d) level of theory in both the neutral and protonated form in aqueous phase.

The reactive ability of the inhibitor is considered to be closely related to their frontier molecular orbitals, the HOMO and LUMO. Higher HOMO energy (E_{HOMO}) of the molecule means a higher electron donating ability to appropriate acceptor molecules with low-energy empty molecular orbital and thus explains the adsorption on metallic surfaces by way of delocalized pairs of π-electrons. E_{LUMO}, the energy of the lowest unoccupied molecular orbital signifies the electron receiving

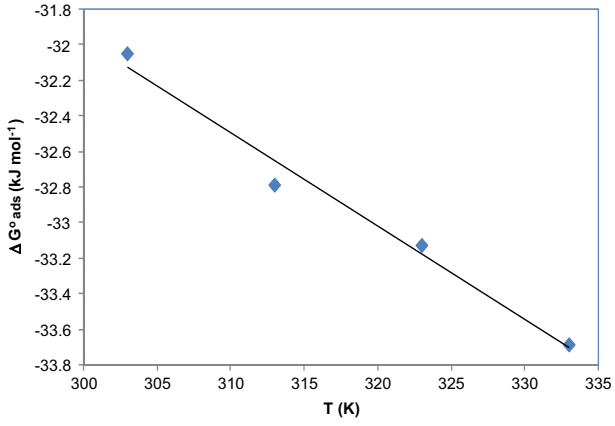

Figure 10 The variation of ΔG^{o}_{ads} with temperature.

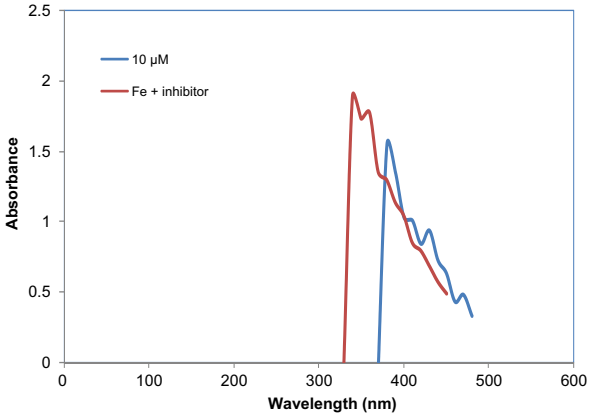

Figure 11 UV-Visible spectra of the solution containing 0.5 M H_2SO_4 (10×10^{-6} M) XION before (blue) and after three days of mild steel immersion (red).

tendency of a molecule. Accordingly, the difference between E_{LUMO} and E_{HOMO} energy levels ($\Delta E = E_{LUMO} - E_{HOMO}$) and the dipole moment (μ) were also determined. The global hardness η is approximated as $\Delta E/2$, and can be defined under the principle of chemical hardness and softness (HSAB) (Khaled, 2010). These parameters also provide information about the reactive behavior of molecules and are presented in Table 5. These theoretical parameters were calculated in the neutral as well as in the protonated form of XION in the aqueous phase.

It could be seen from Figs. 13 and 14 that XION can have different HOMO and LUMO distributions. The HOMO densities were mainly concentrated on the sulphur atom while the LUMO densities were located on the entire xanthione moiety. Thus, unoccupied d-orbitals of Fe atom can accept electrons from inhibitor molecule mainly using the sulphur atom to form a coordinate bond. Also the inhibitor molecule can accept electrons from Fe atom with its anti-bonding orbitals to form back-donating bond. Fig. 15 shows the Mulliken atomic charges calculated for XION. It has been reported that the more negative the atomic charges of the adsorbed centre, the more easily the atom donates its electron to the unoccupied orbital of the metal (Xia et al., 2008). It is clear from Fig. 15 that sulphur and oxygen as well as some carbons atoms carry negative charge centers which could offer electrons to the mild steel surface to form a coordinate bond. It should be noted that there are more negative charge centers in the neutral form of XION than in the protonated form. The highest negative charges are domiciled in O1 and S1. This shows that the two atoms are the probable reactive sites for the adsorption of iron. Thus, the neutral form of XION donates more negative charge to the d-orbitals of Fe than in the protonated form.

Higher values of E_{HOMO} are likely to indicate a tendency of the molecule to donate electrons to appropriate acceptor molecules with low energy or empty electron orbital. It is evident from Table 5 that xanthione has the highest E_{HOMO} in the neutral form and a lower E_{HOMO} in the protonated form. This means that the electron donating ability of XION is weaker in the protonated form. This confirms the experimental results that interaction between XION and mild steel is electrostatic in nature (physisorption). The energy of the LUMO is directly related to the electron affinity and characterizes the susceptibility of the molecule towards attack by nucleophiles. The lower the values of E_{LUMO} are, the stronger the electron accepting abilities of molecules are. It is clear from Table 4 that the protonated form of XION exhibits the lowest $E_{HOMO,}$ making the

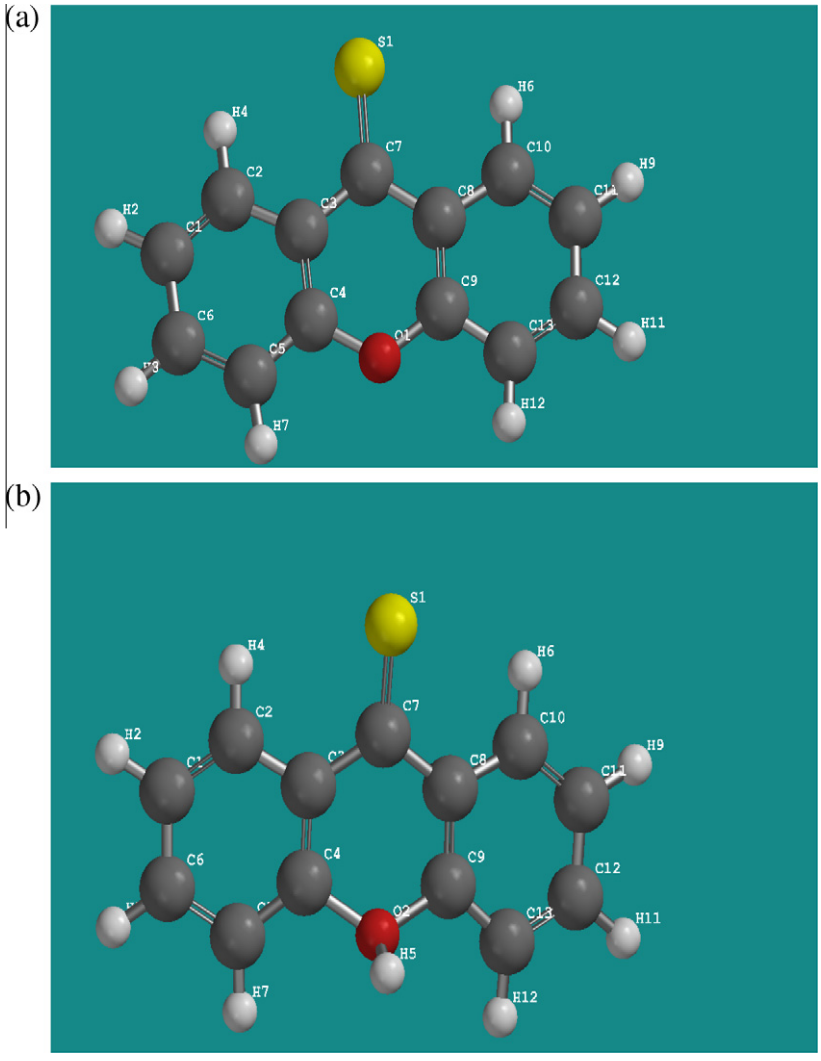

Figure 12 Optimized structure of xanthione (XION) (ball and stick model): (a) neutral molecule and (b) protonated at oxygen.

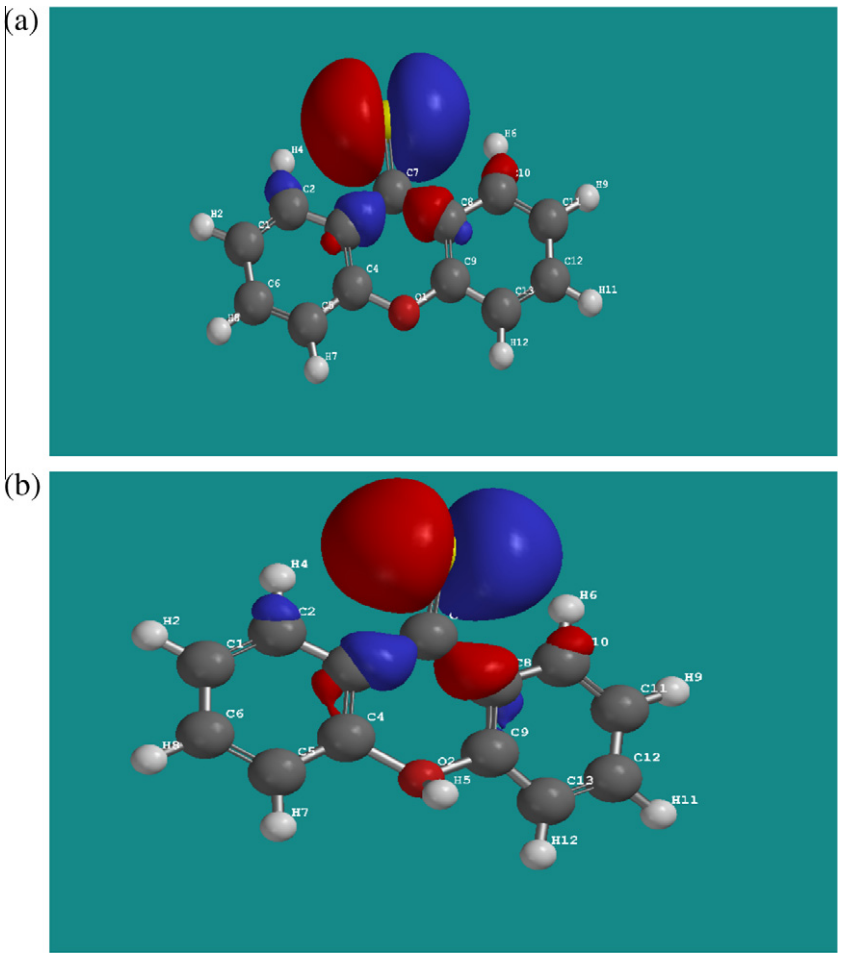

Figure 13 The highest occupied molecular orbital (HOMO) density of xanthione (XION) using DFT at the B3LYP/6-31G (d) basis set level: (a) neutral molecule (b) protonated molecule.

protonated form the most likely form for the interaction of mild steel with xanthione molecule. Low values of the energy gap (ΔE) will provide good inhibition efficiencies, because the excitation energy to remove an electron from the last occupied orbital will be low (Gece, 2008). A molecule with a low energy gap is more polarizable and is generally associated with a high chemical reactivity, low kinetic stability and is termed soft molecule (Dwivedi and Misra, 2010). According to Wang et al. (2007), adsorption of inhibitor onto a metallic surface occurs at the part of the molecule which has the greatest softness and lowest hardness. The result from Table 4 shows that XION in the protonated form has the lowest energy gap and lowest hardness; this agrees with the experimental results that XION could have better inhibitive performance on mild steel surface in the protonated form i.e. through electrostatic interaction between the cation form of XION and the vacant d-orbital of mild steel (physisorption). Moreover, the adsorption of XION on the steel surface using the neutral form also plays a part in the overall inhibiting process. This also agrees well with the value of ΔG^{o}_{ads} and ΔH^{o}_{ads} obtained experimentally. The dipole moment is another important electronic parameter that results from non-uniform distribution of charges on the various atoms in a molecule. It is mainly used to study the intermolecular interactions involving the Van der Waals type dipole-dipole forces etc, because the larger the dipole moment the stronger will be the intermolecular attraction (Dwivedi and Misra, 2010). The dipole moment of XION is highest in the protonated form (4.52 D; 15.07×10^{-30} Cm), which is higher than that of H_2O ($\mu = 6.23 \times 10^{-30}$ Cm). The high value of dipole moment probably increases the adsorption between chemical compound and metal surface (Li et al., 2009). Accordingly, the adsorption of XION molecules can be regarded as a quasi-substitution process between the XION compound and water molecules at the mild steel surface.

3.7. *Mechanism of corrosion inhibition*

A number of mechanistic studies on the anodic dissolution of Fe in acidic solutions have been undertaken, and the hydroxyl accelerated mechanism proposed initially by Bockris and Drazic (1962) and reported by Oguzie (2004) has gained overwhelming acceptance:

$$Fe + H_2O \leftrightarrow FeOH_{ads} + H + e \quad (14)$$

$$FeOH_{ads} \rightarrow FeOH^{+} + e \quad \text{(rate determining step)} \quad (15)$$

$$FeOH^{+} + H^{+} \leftrightarrow Fe^{2+} + H_2O \quad (16)$$

It has been suggested that anions such as Cl^{-}, I^{-}, SO_4^{2-} and S^{2-} may also participate in forming reaction intermediates on the corroding metal surface, which either inhibit or stimulate

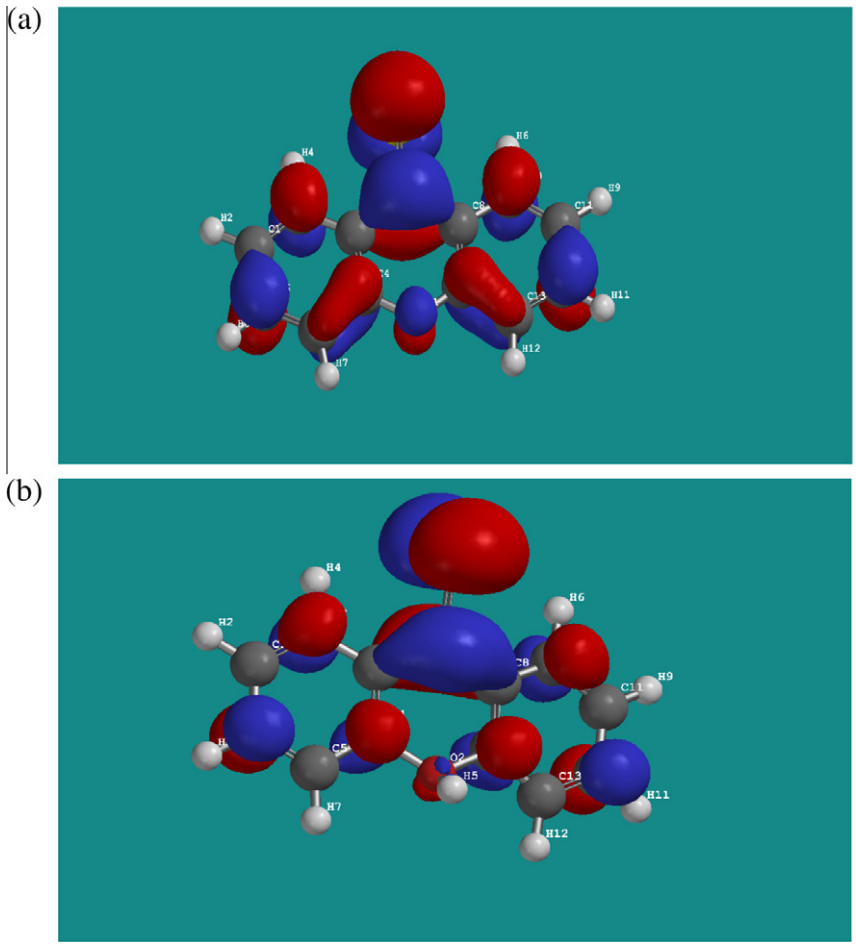

Figure 14 The lowest unoccupied molecular orbital (LUMO) density of xanthione (XION) using DFT at the B3LYP/6-31G (d) basis set level: (a) neutral molecule (b) protonated molecule.

corrosion (Hurlen et al., 1984). It is important to recognize that the suppression or stimulation of the dissolution process is initiated by the specific adsorption of the anions on the metal surface.

According to the Bockris mechanism outlined earlier, Fe electro-dissolution in acidic sulphate solutions depends primarily on the adsorbed intermediate $FeOH_{ads}$. Ashassi-Sorkhabi and Nabavi-Amri (2000) proposed the following mechanism involving two adsorbed intermediates to account for the retardation of Fe anodic dissolution in the presence of an inhibitor:

$$Fe + H_2O \leftrightarrow FeH_2O_{ads} \quad (17)$$

$$FeH_2O_{ads} + M \leftrightarrow FeOH^-_{ads} + H^+ + M \quad (18)$$

$$FeH_2O_{ads} + M \leftrightarrow FeM_{ads} + H_2O \quad (19)$$

$$FeOH^-_{ads} \rightarrow FeOH_{ads} + e \quad \text{(rate determining step)} \quad (20)$$

$$FeM_{ads} \leftrightarrow FeM^+_{ads} + e \quad (21)$$

$$FeOH_{ads} + FeM^+_{ads} \leftrightarrow FeM_{ads} + FeOH^+ \quad (22)$$

$$FeOH^+ + H^+ \leftrightarrow Fe^{2+} + H_2O \quad (23)$$

where M represents the inhibitor species.

Considering the inhomogeneous nature of metallic surfaces resulting from the existence of lattice defects and dislocations, a corroding metal surface is generally characterized by multiple adsorption sites having activation energies and heats of adsorption. Inhibitor molecules may thus be adsorbed more readily at surface active sites having suitable adsorption enthalpies. According to the detailed mechanism above, displacement of some adsorbed water molecules on the metal surface by inhibitor species to yield the adsorbed intermediate FeM_{ads} (Eq. (19)) reduces the amount of the species $FeOH^-_{ads}$ available for the rate determining steps and consequently retards Fe anodic dissolution (Obot and Obi-Egbedi, 2010a; Omar and Mokhtar, 2010).

From the experimental and theoretical results obtained, we note that a plausible mechanism of corrosion inhibition of mild steel in 0.5 M H_2SO_4 by xanthione may be deduced on the basis of adsorption. The adsorption process is affected by the chemical structures of the inhibitor, the nature and charged surface of the metal and the distribution of charge over the whole inhibitor molecule. In general, owing to the complex nature of adsorption and inhibition of a given inhibitor, it is impossible for single adsorption mode between inhibitor and metal surface.

The adsorption and inhibition effect of XION in 0.5 M H_2SO_4 solution can be explained as follows. XION might be protonated in acid solution mainly on the O1 atom (more negative charge centre) as:

$$C_{13}H_8OS + xH^+ \leftrightarrow [C_{13}H_8OHS]^{x+} \quad (24)$$

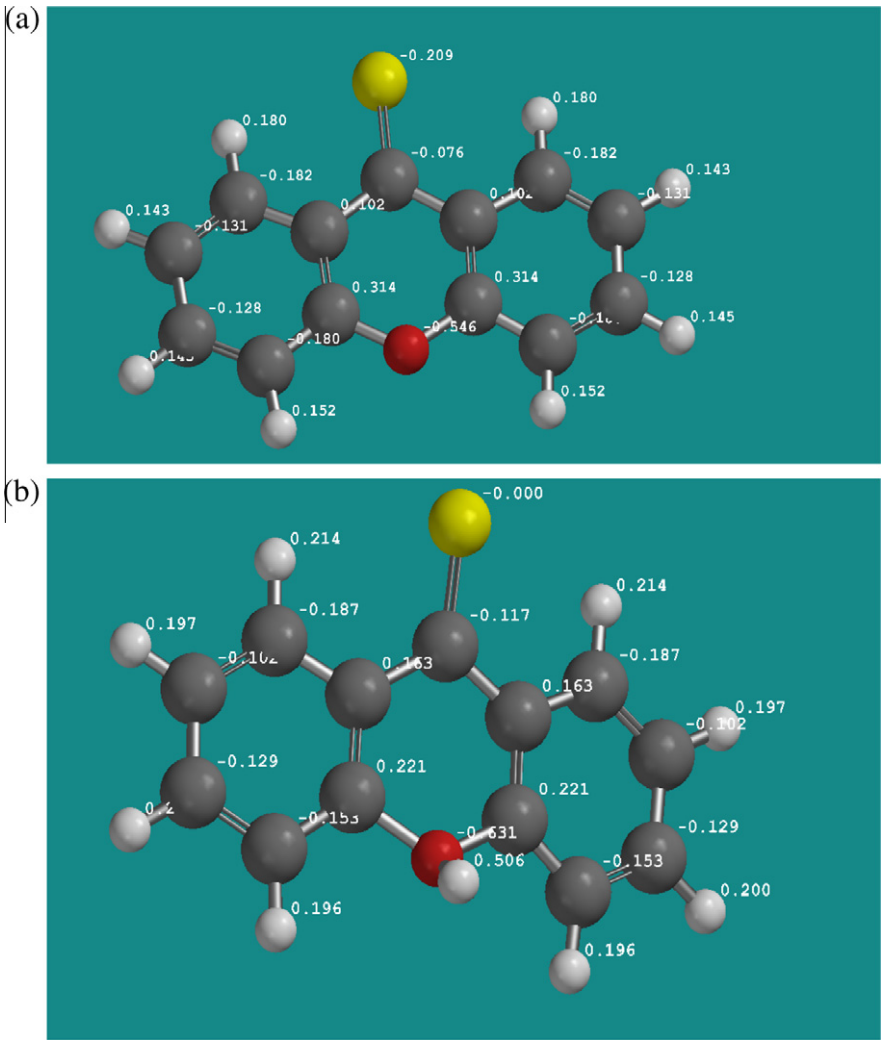

Figure 15 Mulliken charges population analysis of xanthione (XION) using DFT at the B3LYP/6-31G (d) basis set level: (a) neutral molecule (b) protonated molecule.

Table 5 Some molecular properties of xanthione calculated using DFT at the B3LYP/6-31G (d) basis set.

Inhibitor	E_{homo} (eV)	E_{lumo} (eV)	ΔE (eV)	μ (D)	η
XION (neutral form)	−5.71	−2.50	3.21	3.75	1.605
XION (protonated at O1)	−9.78	−6.71	3.07	4.52	1.535

Thus, in aqueous acidic solutions, the XION exists either as neutral molecules or in the form of protonated XION (cations). XION may adsorbed on the metal/acid solution interface by one and/or more of the following ways: (i) electrostatic interaction of protonated XION with already adsorbed sulphate ions, (ii) donor-acceptor interactions between the π-electrons of aromatic ring and vacant d orbital of iron surface atoms, (iii) interaction between unshared electron pairs of O1 and S1 atoms of XION and vacant d orbital of iron surface atoms.

Generally, two modes of adsorption could be considered. In one mode, the neutral XION molecules may be on the surface of mild steel through the chemisorption mechanism involving the displacement of water molecules from the mild steel surface and the sharing of electrons between the heteroatoms and iron. The inhibitor molecule can also adsorb on the mild steel surface on the basis of donor-acceptor interactions between π-electrons of the heterocyclic ring and vacant d-orbitals of surface iron. In another mode, since it is well known that the steel surface bears positive charge in acid solution (Mu et al., 1996), it is difficult for the protonated XION to approach the positively charged mild steel surface (H_3O^+/metal interface) due to the electrostatic repulsion. Thus, the presence of sulphate ions which have excess negative charges in the vicinity of the interface could favour the adsorption of the positively charged inhibitor molecules. The protonated XION could then adsorb through electrostatic interactions between the positively charged molecules and the steel surface which now has

negatively charged sulphate ions on it. Thus there is a synergism between SO_4^{2-} ions and the protonated XION molecules. Similar mechanism has been proposed recently (Ahamad et al., 2010).

5. Conclusions

The following conclusions may be drawn from the study:

1. Xanthione (XION) acts as an inhibitor for the corrosion of mild steel in 0.5 M H_2SO_4. Inhibition efficiency values increase with the inhibitor concentration but decrease with rise in temperature suggesting physical adsorption mechanism. The adsorption of XION on steel surface was found to accord with Langmuir adsorption isotherm model. The adsorption process is spontaneous, exothermic and accompanied with a decrease in entropy of the system from thermodynamic point of view.
2. UV–visible spectrophotometric studies clearly reveal the formation of Fe–XION complex which may be responsible for the observed inhibition.
3. Data obtained from quantum chemical calculations using DFT at the B3LYP/6-31G (d) level of theory were correlated to the inhibitive effect of xanthione. Both experimental and theoretical calculations are in excellent agreement.

References

Abboud, Y., Abourriche, A., Saffaj, T., Berrada, M., Charrouf, M., Bennamara, A., Al-Himidi, N., Hannache, H., 2007. Mater. Chem. Phys. 105, 1.

Abboud, Y., Abourriche, A., Ainane, T., Charrouf, M., Bennamara, A., Tanane, O., Hammouti, B., 2009. Chem. Eng. Comm. 196, 788.

Abdallah, M., El-Naggar, M.M., 2001. Mater. Chem. Phys. 71, 291.

Abdel-Gaber, A.M., Abd-ElNabey, B.A., Sidahmed, I.M., El-Zayady, A.M., Saadawy, M., Abboud, Y., Abourriche, A., Saffaj, T., Berrada, M., Charrouf, M., Bennamara, A., Hannache, H., 2009. Desalination 237, 175.

Afidah, A.R., Kassim, J., 2008. Recent Patents Mater. Sci. 1, 223.

ASTM G1-72, 1990. Practice for Preparing, Cleaning and Evaluating Corrosion Test Specimens.

Ahamad, I., Prasad, R., Quraishi, M.A., 2010. Corros. Sci. 52, 1472.

Ahamad, I., Quraishi, M.A., 2010. Corros. Sci. 52, 651.

Ashassi-Sorkhabi, H., Nabavi-Amri, S.A., 2000. Acta Chim. Slov. 47, 512.

Behpour, M., Ghoreishi, S.M., Gandomi-Niasar, A., Soltani, N., Salavati-Niasari, M., 2009. J. Mater. Sci. 44, 2444.

Bentiss, F., Lebrini, M., Lagrenee, M., 2005. Corros. Sci. 47, 2915.

Bentiss, F., Traisnel, M., Gengembre, L., Lagrenee, M., 1999. Appl. Surf. Sci. 152, 237.

Bockris, J.O.M., Drazic, D., 1962. Electrochim. Acta 7, 293.

Bockris J.O.M., Reddy, A.K.N., 1977. Modern Electrochemistry, vol. 2. Plenum Press, New York, p. 1267.

Bouklah, M., Hammouti, B., Lagrenee, M., Bentiss, F., 2006. Corros. Sci. 48, 2831.

Donahue, F.M., Nobe, K., 1965. J . Electrochem. Soc. 112, 886.

Dwivedi, A., Misra, N., 2010. Der Pharma Chem. 2 (2), 58.

Ebenso, E.E., Arslan, T., Kandemirli, F., Caner, N., Love, I., 2010. Int. J. Quant. Chem. 110, 1003.

Elmorsi, M.A., Hassanein, M.A., 1999. Corros. Sci. 41, 2337.

Fouda, A.S., Abdallah, M., Ahmed, I.S., Eissa, M., 2010. Arab. J. Chem.. doi:10.1016/j.arabjc.2010.08.020.

Gece, G., 2008. Corros. Sci. 50, 2981.

Gopalakrishnan, G., Banumathi, B., Suresh, G., 1997. J. Nat. Prod. 60 (5), 519.

Guan, N.M., Xueming, I., Fei, I., 2004. Mater. Chem. Phys. 86, 59.

Herrag, L., Hammouti, B., Elkadiri, S., Aouniti, A., Jama, C., Vezin, H., Bentiss, F., 2010. Corros. Sci. doi:10.1016/j.corsci.2010.05.024.

Hurlen, T., Lian, H., Odegard, O.S., Valand, T., 1984. Electrochim. Acta 29, 579.

Ignatushchenko, M.V., Winter, R.W., Riscoe, M., 2000. Am. J. Trop. Med. Hgy 62 (1), 77.

Khadom, A.A., Yaro, A.S., Kadum, A.H., 2010. J. Taiwan Inst. Chem. Eng. 41, 122.

Khaled, K.F., Abdel-Rehim, S.S., Saker, G.B., 2010. Arab. J. Chem.. doi:10.1016/j.arabjc.2010.08.015.

Khaled, K.F., 2010. Corros. Sci. doi:10.1016/j.corsci.2010.05.039.

Kissi, M., Bouklah, M., Hammouti, B., Benkaddour, M., 2006. Appl. Surf. Sci. 252, 4190.

Lagrenee, M., Mernari, B., Bouanis, M., Traisnel, M., Bentiss, F., 2002. Corros. Sci. 44, 573.

Landau, L.D., Lifshitz, E.M., 1980. Statistical Physics. Pergamon Press, Oxford, p. 107.

Lashkari, M., Arshadi, M.R., 2004. J. Chem. Phys. 299, 131.

Lee, C., Yang, W., Parr, R.G., 1988. Phys. Rev. B 37, 785.

Li, X., Deng, S., Fu, H., 2010. Prog. Org. Coat. 67, 420.

Li, X., Deng, S., Fu, H., Li, T., 2009. Electrochim. Acta 54, 4089.

Machnikova, E., Whitmire, K.H., Hackerman, N., 2008. Electrochim. Acta 53, 6024.

Mansfeld, F., 1987. Corrosion Mechanism. Marcel Dakkar, New York, NY, p. 119.

Mu, G.N., Zhao, T.P., Liu, M., Gu, T., 1996. Corrosion 52, 853.

Musa, A.Y., Khadom, A.A., Kadhum, H., Mohamad, A.B., Takriff, M.S., 2010. J. Taiwan Inst. Chem. Eng. 41, 126.

Noor, E.A., Al-Moubaraki, A.H., 2008. Mater. Chem. Phys. 110, 145.

Obi-Egbedi, N.O., Obot, I.B., 2010. Arab. J. Chem.. doi:10.1016/j.arabjc.2010.08.004.

Obot, I.B., 2009. Portugaliae Electrochim. Acta 27(5), 539.

Obot, I.B., Obi-Egbedi, N.O., 2009. Corros. Sci. 52, 276.

Obot, I.B., Obi-Egbedi, N.O., 2010a. Corros. Sci. 52, 198.

Obot, I.B., Obi-Egbedi, N.O., 2010b. Curr. Appl. Phys.. doi:10.1016/j.cap. 2010.08.007.

Obot, I.B., Obi-Egbedi, N.O., Umoren, S.A., 2009. Int. J. Electrochem. Sci. 4, 863.

Oguzie, E.E., 2004. Mater. Chem. Phys. 87, 212.

Omar, B., Mokhtar, O., 2010. Arab. J. Chem.. doi:10.1016/j.arabjc.2010.07.016.

Pavithra, M.K., Venkatesha, T.V., Vathsala, K., Nayana, K.O., 2010. Corros. Sci. doi:10.1016/j.corsci.2010.07.034.

Pedraza-Chaverri, J., Cardenas-Rodriguez, N., Orozco-Ibarra, M., Perez-Rojas, J.M., 2008. Food Chem. Toxicol 46 (10), 3227.

Rangelov, S., Mircheva, V., 1996. Corros. Sci. 38, 301.

Shao, Y., Molnar, L.F., Jung, Y., Kussmann, J., Ochsenfeld, C., Brown, S.T., Gilbert, A.T.B., Slipehenko, L.V., Levehenko, S.V., O'Neill, D.P., DiStasio Jr., R.A., Lochan, R.C., Wang, T., Beran, G.J.O., Besley, N.A., Herbert, J.M., Lin, C.Y., Van Voorhis, T., Chien, S.H., Sodt, A., Steele, R.P., Rassolov, V.A., Maslen, P.E., Korambath, P.P., Adamson, R.D., Austin, B., Baker, J., Byrd, E.F.C., Dachsel, H., Doerksen, R.J., Dreuw, A., Dunietz, B.D., Dutoi, A.D., Furlani, T.R., Gwaltney, S.R., Heyden, A., Hirata, S., Hsu, C.P., Kedziora, G., Khalliulin, R.Z., Klunzinger, P., Lee, A.M., Lee, M.S., Liang, W.Z., Lotan, I., Nair, N., Peters, B., Proynov, E.I., Pieniazek, P.A., Rhee, Y.M., Ritchie, J., Rosta, E., Sherrill, C.D., Simmonett, A.C., Subotnik, J.E., Woodcock III., H.L., Zhang, W., Bell, A.T., Chakraborty, A.K., Chipman, D.M., Keil, F.J., Warshel, A., Hehre, W.J., Schaefer, H.F., Kong, J., krylov, A.I., Gill, P.M.W., Head-Gordon, M.Spartan,06 Wavefunction, Inc. Irvine, CA, 2006. Phys. Chem. Chem. Phys. 8, 3172.

Sahin, M., Bilgic, S., Yilmaz, H., 2002. Appl. Surf. Sci. 195, 1.

Sein, L.T., Wei, Y., Jansen, S.A., 2001. Comput. Theor. Polym. Sci. 11, 83.

Sherif, E.M., Park, S.M., 2005. J. Electrochem. Soc. 152, B428.
Singh, A.K., Quraishi, M.A., 2010. Corros. Sci. 52, 152.
Solmaz, R., 2010. Corros. Sci. doi:10.1016/j.corsci.2010.06.001.
Solmaz, R., Kardas, G., Culha, M., Yazici, B., Erbil, M., 2008a. Electrochim. Acta 53, 5941.
Solmaz, R., Kardas, G., Yazici, B., Erbil, M., 2008b. Colloids Surf. A: Physicochem. Eng. Aspects 312, 7.
Szauer, T., Brand, A., 1981. Electrochim. Acta 26, 245.
Umoren, S.A., Obot, I.B., Obi-Egbedi, N.O., 2009b. J. Mater. Sci. 44, 274.
Umoren, S.A., Obot, I.B., Ebenso, E.E., Obi-Egbedi, N.O., 2009a. Desalination 247, 561.
Villamil, R.F.V., Corio, P., Rubim, J.C., Agostinho, S.M.L., 1999. J. Electroanal. Chem. 472.
Wang, H.L., Fan, H.B., Zheng, J.S., 2002. Mater. Chem. Phys. 77, 655.
Wang, H., Wang, X., Wang, H., Wang, L., Liu, A., 2007. J. Mol. Model. 13, 147.
Xia, S., Qiu, M., Yu, L., Liu, F., Zhao, H., 2008. Corros. Sci. 50, 2021.